Supplementary Information

TLR3 forms a laterally aligned multimeric complex along double-stranded RNA for efficient signal transduction

Authors

Kentaro Sakaniwa[1], Akiko Fujimura[1], Takuma Shibata[2], Hideki Shigematsu[3], Toru Ekimoto[4], Masaki Yamamoto[3], Mitsunori Ikeguchi[4], Kensuke Miyake[2], Umeharu Ohto[1]* and Toshiyuki Shimizu[1]*

***Corresponding author:**

Umeharu Ohto (U.O.)　E-mail: umeji@mol.f.u-tokyo.ac.jp

Toshiyuki Shimizu (T.S.)　E-mail: shimizu@mol.f.u-tokyo.ac.jp

This file includes:

Supplementary Figure legends 1-7

Supplementary Table 1

Supplementary Table 1 Cryo-EM data collection, refinement, and validation statistics

	Mouse TLR3 (26-705)-dsRNA (90 bp) (EMD-32599, PDB 7WM4)
Data collection and processing	
Magnification	60,000
Voltage (kV)	300
Electron exposure (e^{-}/Å^2)	50
Defocus range (μm)	-1.4 to -2.4
Pixel size (Å)	0.752
Symmetry imposed	*C*2
Initial particle images (no.)	10,866,015
Final particle images (no.)	274,002
Map resolution (Å)	3.2
FSC threshold	0.143
Refinement	
Model resolution (Å)	3.2
FSC threshold	0.5
Map sharpening *B* factor (Å^2)	95.9
Model composition	
Non-hydrogen atoms	25,848
Protein residues: TLR3	2,658
Nucleotides: dsRNA	162
Glycans: NAG, BAM	82
B factors (Å^2)	
TLR3	208.28
DsRNA	229.64
Glycans	232.76
R.m.s. deviations	
Bond lengths (Å)	0.002
Bond angles (°)	0.524
Validation	
MolProbity score	1.85
Clashscore	9.68
Rotamer outliers (%)	0.00
Ramachandran plot	
Favored (%)	95.11
Allowed (%)	4.81
Outliers (%)	0.08

(a)

12,825 movie stacks (pixel size = 0.752 Å)
(Data processing with cryoSPARC)
↓ Patch motion
↓ Patch CTF
↓ Curate exposures
↓ Template picker
6,581,096 particles →

↓ Extract (4.51 Å/px, box = 361.0 Å)
↓ 2D classification (22 subsets)
↓ Remove duplicates
↓ Extract (1.50 Å/px, box = 391.0 Å)
1,211,275 particles
↓ Heterogeneous refinement, 2 classes
617,012 particles
↓ Heterogeneous refinement, 2 classes
543,476 particles ←

↓ Extract (4.51 Å/px, box = 361.0 Å)
↓ Heterogeneous refinement, 16 subsets, 2classes
↓ Remove duplicates
↓ Extract (1.13 Å/px, box = 406.1 Å)
770,875 particles
↓ Heterogeneous refinement, 2 classes
537,283 particles
↓ Heterogeneous refinement, 2 classes
431,429 particles

↓ Remove duplicates
650,454 particles
↓ Heterogeneous refinement, 2 classes
344,106 particles
↓ NU Refinement (C2): 3.22 Å (FSC = 0.143)

Representative micrograph

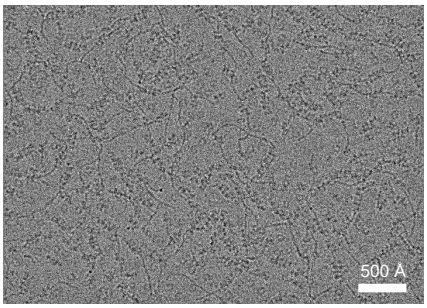

Defocus tilt angle (curate exposures)

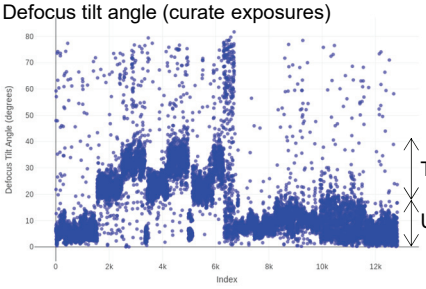

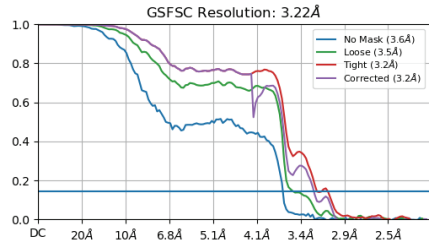

2D class images (untilt + tilt data)

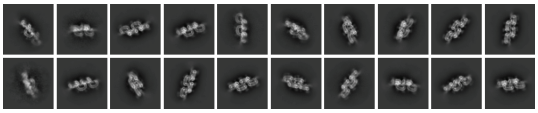

2D class images (untilt data only)

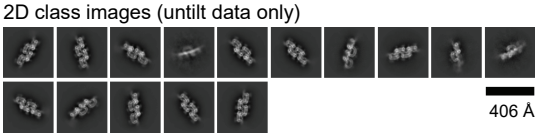

Angular distribution

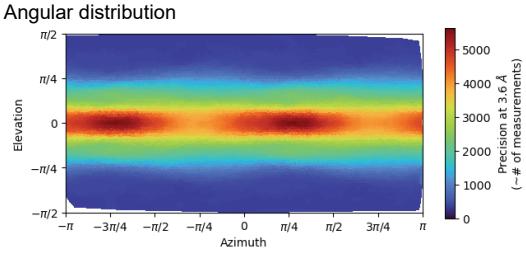

Final map colored by local resolution
(unsharpened)

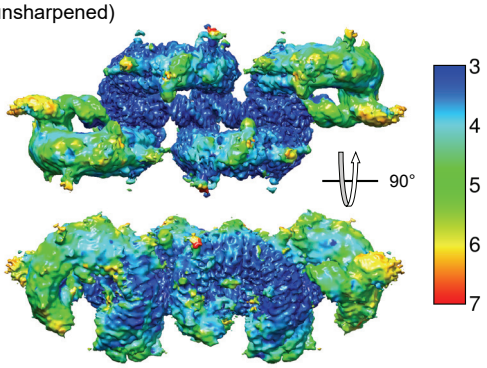

Model to map FSC curve

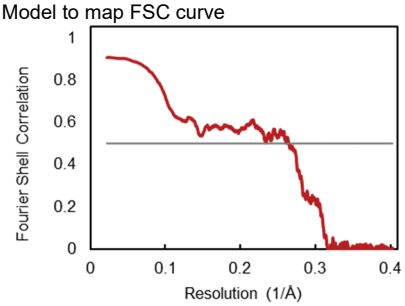

(b)

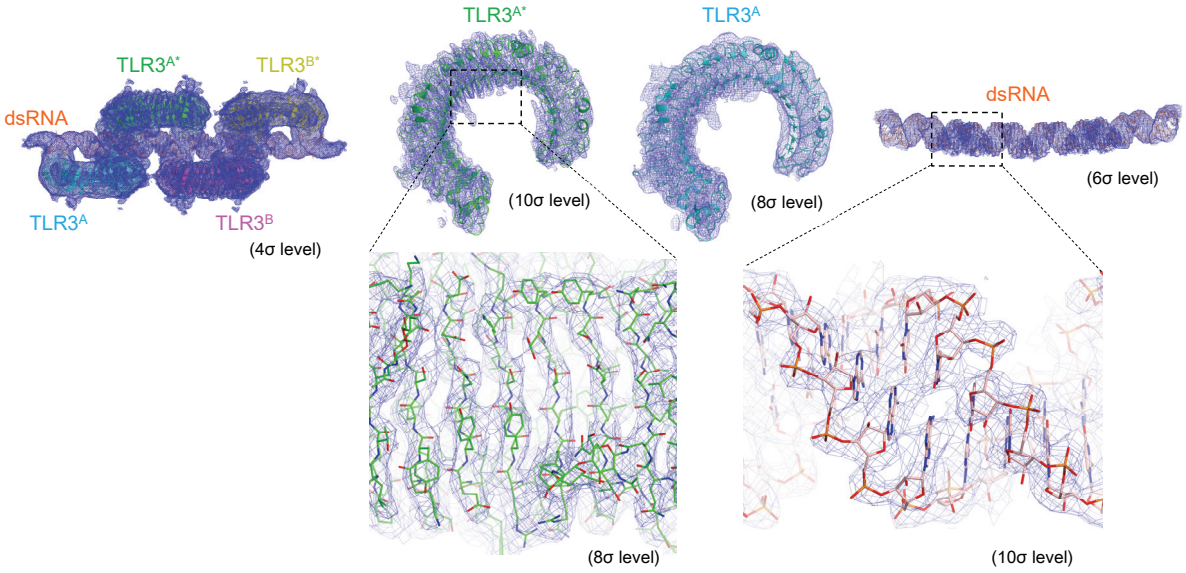

Supplementary Fig. 1 Cryo-EM data processing of the mouse TLR3-dsRNA (90 bp) complex.

(a) Cryo-EM data analyses. Cryo-EM data processing workflow, a representative motion-corrected micrograph, defocus tilt angle, 2D classification images, gold-standard FSC curve (resolution cut-off at FSC = 0.143) and angular distribution of the final 3D reconstitution, the final 3D-map colored according to the local resolution, and model to map FSC curve are shown.

(b) Representative cryo-EM density maps of mouse TLR3-dsRNA (90 bp) complex. The map levels are indicated in each panel.

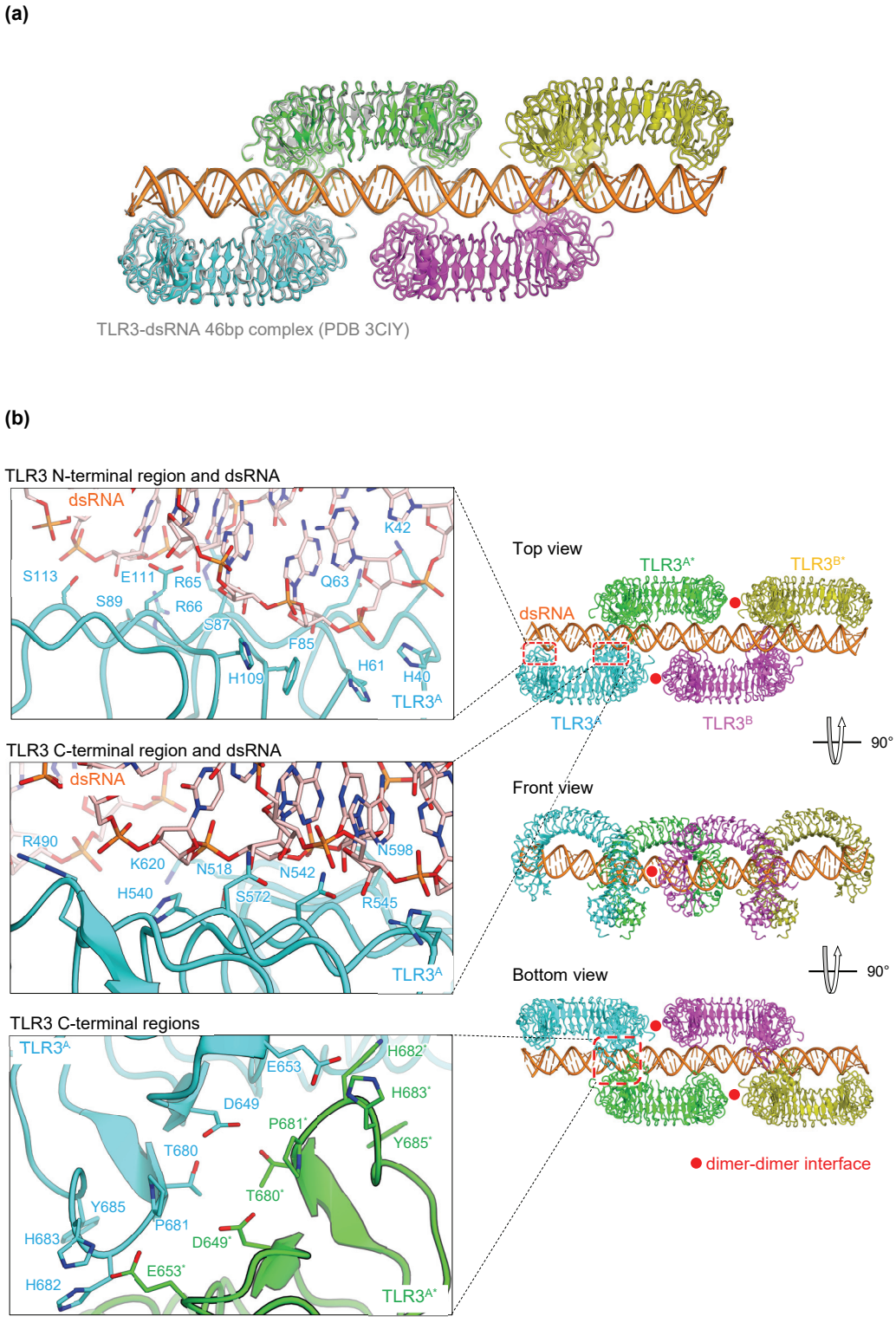

Supplementary Fig. 2 TLR3 dimer unit in the mouse TLR3-dsRNA (90 bp) complex.

(a) Structural comparison of the TLR3 dimer unit between the mouse TLR3-dsRNA (90 bp) complex (this study) and mouse TLR3-dsRNA (46 bp) complex colored gray (PDB 3CIY).

(b) The magnified views of the TLR3-dsRNA interfaces (left top and middle) and TLR3-TLR3* interface (left bottom) in the mouse TLR3-dsRNA (90 bp) complex, indicated by the dashed rectangles in the right panel. The residues involved in the TLR3-dsRNA or TLR3-TLR3* interactions are shown with sticks. The dimer-dimer interfaces are indicated by the red circle.

dsRNA (fold)	12.9	4.3	1.4	0.5
tetramer	1778	1468	3257	6642
dimer	12570	14174	14629	3677
dimer + dimer	N.D.	N.D.	N.D.	494
tetramer + dimer	N.D.	N.D.	N.D.	310
tetramer (%)	12.4	9.4	18.2	58.3

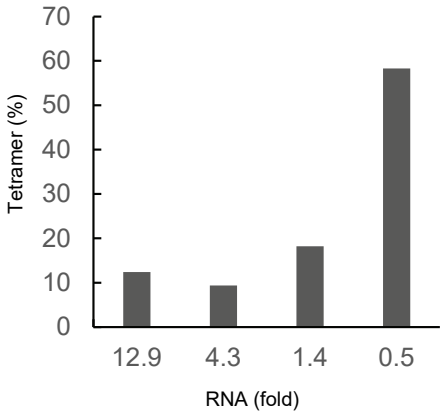

Supplementary Fig. 3 Tetramer formation of TLR3 in the presence of different concentrations of dsRNA.

The cryo-EM 2D class-averaged analyses were performed using WT TLR3 with different concentrations of 90 bp dsRNA.

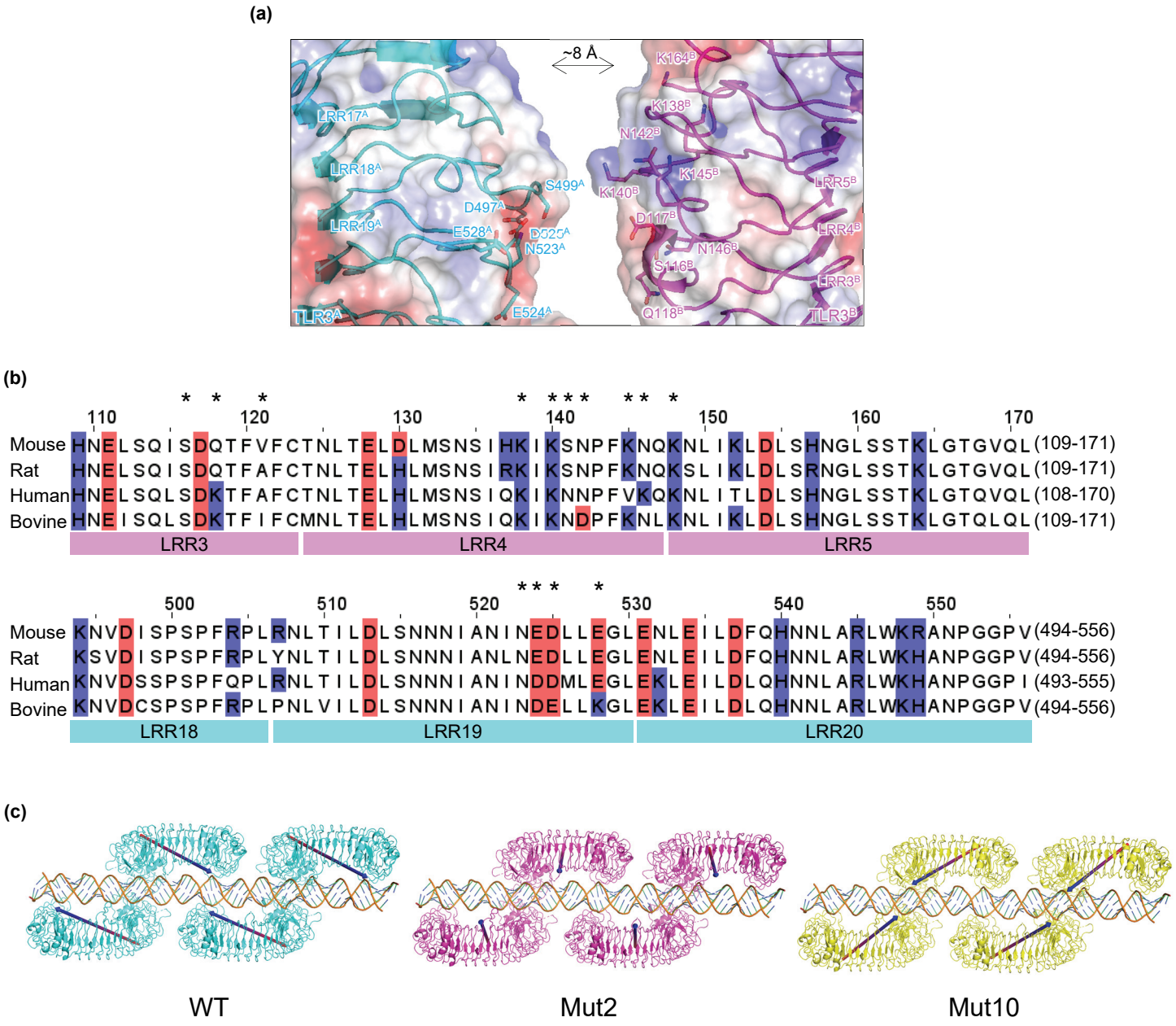

Supplementary Fig. 4 Multiple sequence alignment of TLR3.

(a) The close-up view of the dimer-dimer interface with the transparent electrostatic surface potentials map.

(b) Multiple sequence alignment of the mouse, rat, human, and bovine TLR3. The sequences of LRR3 to LRR5 (top) and LRR18 to LRR20 (bottom) are shown. The positively or negatively charged residues are highlighted with blue or red, respectively. The residues to which the mutations were introduced in this study are marked with asterisks (*).

(c) Dipole moment of WT or mutant TLR3 (Mut2, Mut10). Dipole moment is shown by the arrow.

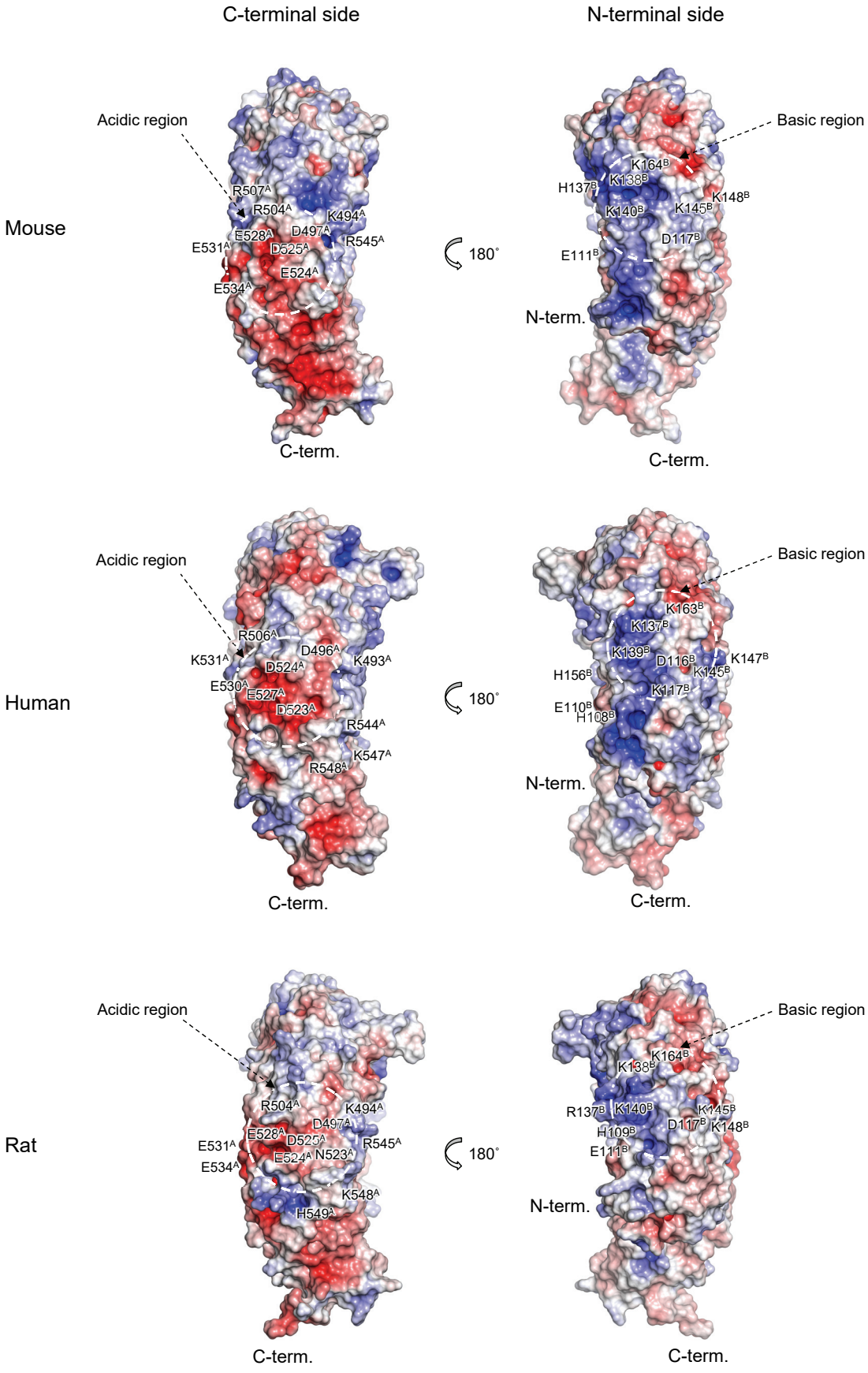

Supplementary Fig. 5 The electrostatic surface potentials of TLR3.

The electrostatic surface potentials of the convex surfaces of the C-terminal regions (left) and the N-terminal regions (right) for the mouse (PDB 3CIY) (top), human (PDB 2A0Z) (middle), and rat (Alphafold database) (bottom) TLR3 are shown. The positively- or negatively-charged regions near the dimer-dimer interface from this study are indicated by white dashed circles.

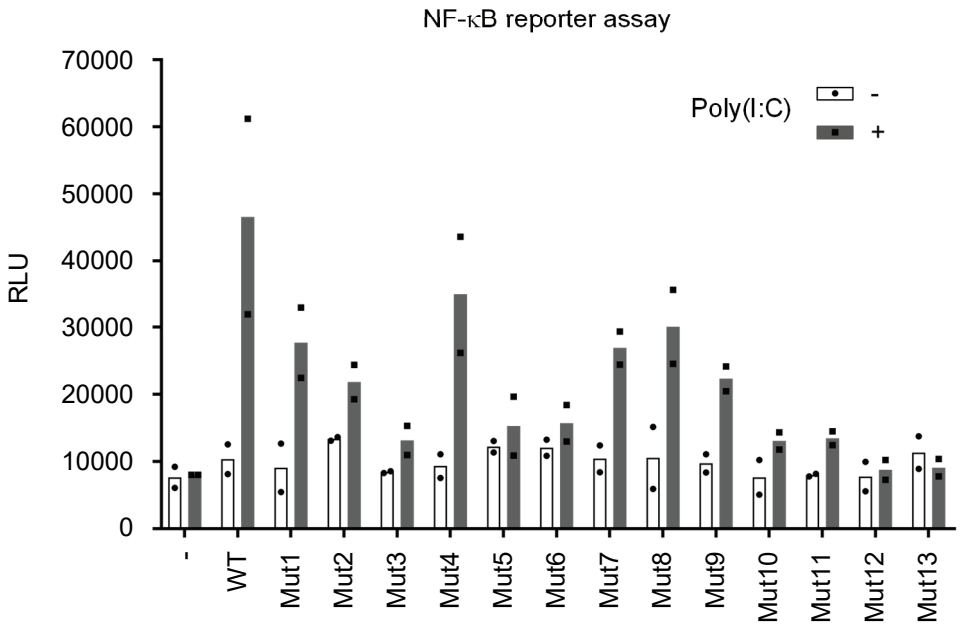

Supplementary Fig. 6 NF-κB reporter assay of multimerization-defective TLR3 mutants.

WT or mutant TLR3-expressing HEK293T cells were stimulated with 1 μg/mL poly (I:C) for 6 h and analyzed by NF-κB reporter assay. Bar plots are mean of n = 2 independent experiments.

(a)

>80 movie stacks x2 from different grids (pixel size = 0.83 Å)
Data processing with Relion
↓ Patch motion
↓ Patch CTF
↓ Autopicking with the references
↓ Extract (binning 6, box size = 480 Å)
↓ 2D classification
↓ Re-extract (binning 4, box size = 480 Å)
↓ 2D classification
↓ Re-extract (binning 3, box size = 480 Å)
↓ 2D classification (3 rounds)
↓ Particle selection to exclude duplicate particles
↓ Re-extract (binning 3, box size = 480 Å)
↓ 2D classification (30 classes) = Fig. 4a

2D references

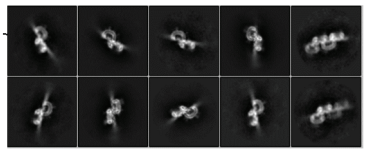

(b)

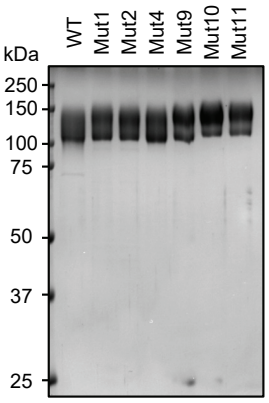

(c)

WT

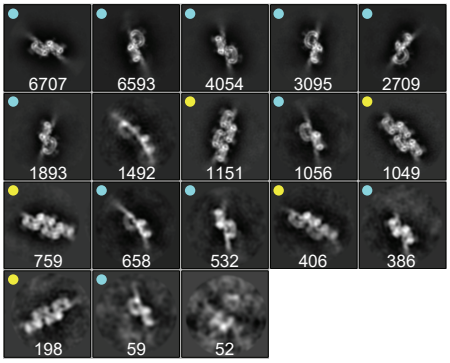

Mut1

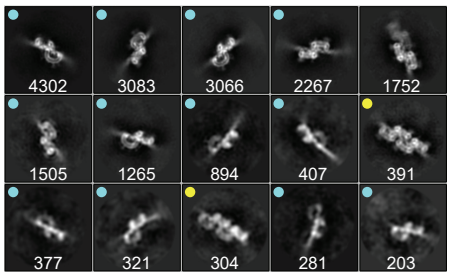

Mut2

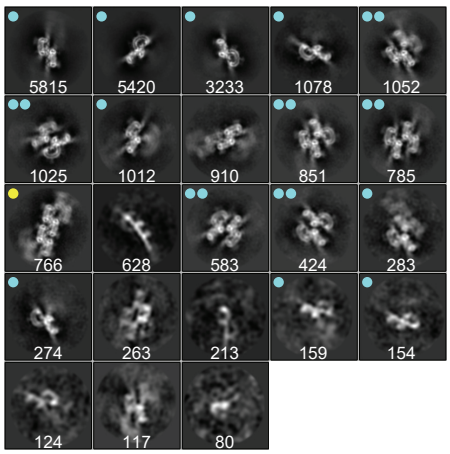

Mut4

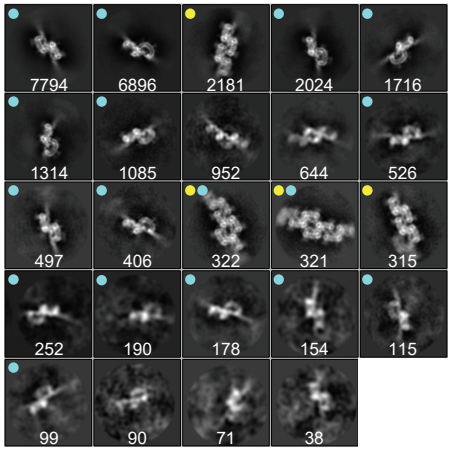

Mut9

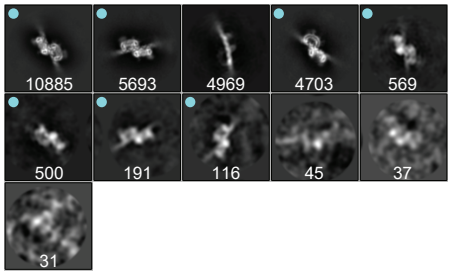

Mut10

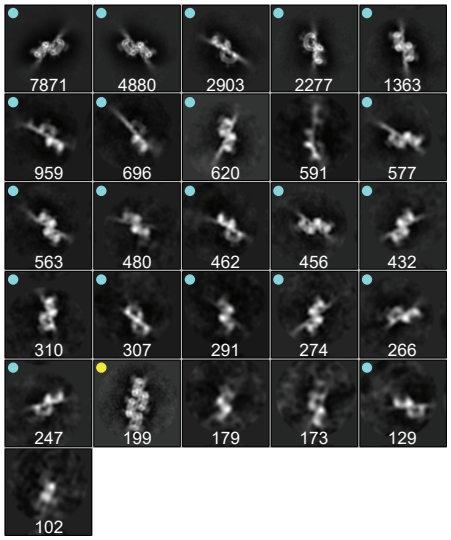

Mut11

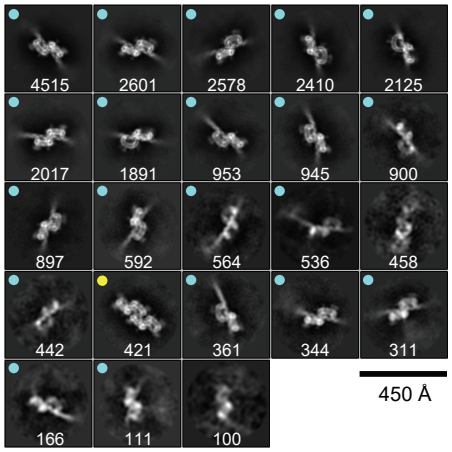

(d)

400 movie stacks (pixel size = 0.83 Å)
(data processing with cryoSPARC)
↓ Patch motion
↓ Patch CTF
↓ Template picker
449,865 particles
↓ Extract (1.245 Å/px, box = 249 Å)
↓ 2D classification
240,455 particles
↓ Heterogeneous refinement, 2 classes
122,126 particles
↓ NU Refinement (C2): 3.24 Å (FSC = 0.143)

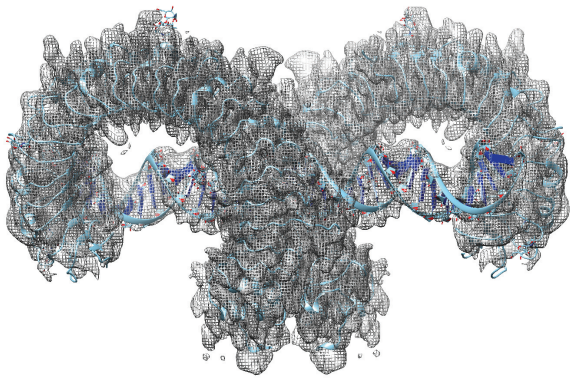

Supplementary Fig. 7 Cryo-EM analyses of multimerization-defective TLR3 mutants.

(a) The procedure of cryo-EM 2D analyses.

(b) The purified recombinant TLR3 mutants. The purified proteins were analysed by SDS-PAGE followed by Coomassie Brilliant Blue staining. Representative gel image in many trials is shown.

(c) Cryo-EM analyses of multimerization-defective TLR3 mutants in the presence of 90 bp dsRNA. 2D classification images in Fig. 3b are shown along with the number of particles in each class. The dimer and tetramer classes are indicated with light blue and yellow dot, respectively.

(d) Cryo-EM structure of TLR3 Mut10 (S116E, Q118E, K138E, K140E, N142E, K145E, N146E). Mouse TLR3-dsRNA 46bp complex (PDB 3CIY) is superposed onto the cryo-EM map of Mut10.